Small-Angle Neutron Scattering from a Polyurethane Block Copolymer

John A. Miller and Stuart L. Cooper*

Department of Chemical Engineering, University of Wisconsin—Madison, Madison, Wisconsin 53706

Charles C. Han

Polymer Division, National Bureau of Standards, Washington, D.C. 20234

Gerfried Pruckmayr

Chemicals and Pigments Division, E. I. du Pont de Nemours and Co., Experimental Station, Wilmington, Delaware 19898. *Received July 13, 1983*

ABSTRACT: Small-angle neutron scattering (SANS) experiments were performed on a series of polyether–polyurethane block copolymers. The samples possessed the same chemical composition but differed in the percentage of polyether soft segments that were completely deuteriolabeled. The level of labeling covered a wide range, from no labeling up to 30% of the total polyether chains. At the highest level of deuteration, little interphase scattering occurs and the coherent portion of the scattering is dominated by the interchain scattering. The single-chain scattering functions extracted from the scattering data yield a radius of gyration for the soft segment that is substantially larger than that reported for the polyether homopolymer in a Θ solvent.[36] Thus the soft segment chains in this lamellar block copolymer are in a somewhat extended conformation. Results of other work on a styrene/isoprene lamellar block copolymer indicate a similar chain conformation.[23] Experimentally it was found that the technique of matching the interphase contrast yielded the single-chain scattering function with greater accuracy than did the subtraction method. In addition, the smearing effects of wavelength polydispersity and collimation were analyzed. For this experiment, neither smearing phenomenon had any significant effect on the scattering data.

Introduction

Small-angle neutron scattering (SANS) has become an important new tool in the investigation of polymer structure. This is primarily because the experimenter can preferentially label the polymer with deuterium, which dramatically changes the neutron contrast factor, the coherent scattering length density. While an equivalent labeling substitution in X-ray scattering invariably alters the chemistry of the system, the deuterium substitution has little or no effect on the chemistry of the polymer.

Small-angle neutron scattering was first used by Ballard et al.[1] to study the conformation of deuterated polystyrene chains in a hydrogenous polystyrene matrix. They found that the chains in the bulk, amorphous sample possessed the same conformation as when the chains are in a Θ solvent, confirming the hypothesis made by Flory years earlier[2] that polymer chains in an amorphous homopolymer are in a random flight configuration. Subsequent work on other amorphous homopolymers supported this hypothesis.[3–6] Reviews by Higgins and Stein[7] and Richards[8] summarize the SANS results in this area.

SANS has also been used extensively to examine chain conformation in semicrystalline homopolymers. The principle question that SANS has addressed is the reentry mechanism of the chain as it returns into the crystalline lamellae. Both an adjacent reentry model and a random, or switchboard, reentry model have been proposed. Schelten et al.[9] and others[10,11] report that the chain conformation of polyethylene that has been rapidly quenched from the molten state suggests a random reentry trajectory. However, when polyethylene is slowly cooled from the melt, any deuterated molecules tend to segregate, thus rendering the samples useless for neutron scattering.[12] Polypropylene does not undergo isotopic segregation during a slow cool from the melt. Ballard et al.[13] studied a polypropylene sample under these conditions and found that the chain conformation supported a random reentry model. Sadler and Keller[14] and Summerfield et al.[15] have reported evidence for adjacent reentry in polyethylene slowly crystallized from solution. Krimm[16] has gathered evidence for adjacent reentry in polyethylene by using infrared spectroscopy. It appears that the reentry mechanism is subject to the preparation method of the sample. SANS has been used to support both of these possibilities, and it appears that the mechanism is kinetically controlled. To date, no temperature–time studies using SANS have been carried out to resolve this question.

An analogous situation exists for block copolymers. The questions here are how the polymers chains enter and exit the individual domains, and what configuration the chains possess within the domain structure. Two possibilities for the chain conformation in the individual phases are shown in Figure 1. The models may be referred to as the extended-chain conformation and the random flight, or Gaussian, conformation. Recently, Koberstein[17] and Jahshan and Summerfield[18,19] have independently derived the equations necessary for the extraction of the single-chain scattering from chains in one phase of a two-phase system. The experimental technique for determining the single-chain scattering involves obtaining the scattering data from two samples with identical morphology; one sample is an unlabeled control and the other has one of the phases partially labeled with deuterated chains. The unlabeled scattering intensity is weighted by a ratio of contrast factors, then subtracted from the labeled sample scattering intensity, thus yielding the single-chain scattering. This technique will be discussed in more detail later.

Prior to the development of the above-mentioned theory, Richards and Thomason[20] reported the z-average radius of gyration of the styrene blocks in a styrene/isoprene block copolymer which exhibited spherical styrene domains. They reported the size of the styrene block to be the same as that reported by Notley and Debye,[21] within

0024-9297/84/2217-1063$01.50/0

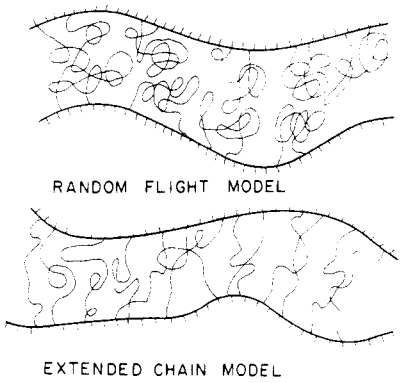

Figure 1. Diagram of two possible extreme conformations of the chain trajectory in a lamellar block copolymer.

experimental error, for polystyrene of the same block length in a Θ solvent as measured by light scattering. These data suggest the styrene chains in the block copolymer approximate the random coil geometry; however, the authors did not state this. The styrene and the deuteriostyrene blocks have number average molecular weights of 9300 and 17 300, respectively. Tangari et al.[22] discuss the problems associated with mismatched block lengths and the errors it can introduce in the data analysis and interpretation.

Hadziioannou et al.[23] investigated the chain conformation of the styrene blocks in a highly regular lamellar styrene/isoprene block copolymer. By carefully aligning the plane of the lamellar surfaces perpendicular to the incident neutron beam, almost all of the interphase scattering due to the lamellar structure was eliminated. This left only the single-chain scattering as the prominent feature of the coherent portion of the scattering. Using Guinier's method[24] to interpret the single-chain scattering at low angles, the authors found that the radius of gyration of the styrene block projected onto the plane of the lamellar surface was considerably smaller than expected for a random coil. This led to the conclusion that the chains are in a somewhat extended conformation perpendicular to the lamellae, similar in outline to a cylinder oriented perpendicular to the lamellae.

Bates et al.[25] were the first to apply the method of Koberstein and Jahshan and Summerfield to a block copolymer system. They investigated the chain conformation of the butadiene block in a styrene/butadiene block copolymer which exhibited spherical butadiene domains. The level of deuteration chosen was such that the contrast between the styrene phase and the partially deuterated butadiene phase was essentially zero. Hence, the coherent portion of the scattering was dominated by the single-chain scattering. The level of deuteration in this sample was relatively high, considerably higher than the concentration normally considered dilute in light scattering. However, Akcasu et al.[26] and Wignall et al.[27] have shown that in neutron scattering experiments, the experimentally determined radius of gyration is fairly independent of the level of deuteriolabeling. Thus one can use high levels of labeling in order to improve the SANS contrast without being concerned by the possible introduction of erroneous results caused by the higher concentration. The results obtained by Bates et al. show that the butadiene chains exist in the random coil conformation.

In this contribution, the chain conformation of a polyether–polyurethane is investigated. In a small-angle X-ray scattering (SAXS) study of similar materials, Van Bogart[28] found that these systems exhibit a lamellar microstructure. It was thought that a SANS study of these lamellar hard domain polyurethanes might resolve the conformational question relating to the flexible polyether soft segments graphically illustrated in Figure 1. Polyurethane elastomers are block copolymers of the $(AB)_n$ type, consisting of alternating rigid and flexible sequences. The hard segments are typically composed of short sequences of diisocyanate/diol or diisocyanate/diamine repeat units. The soft segments are either polyether, polyester, or polyalkyl macroglycols. At service temperatures, the soft segments are well above their glass transition temperature, imparting the rubbery characteristics to the material. In the solid state, the segments separate into individual phases, with some degree of interphase mixing. The hard domains act as multifunctional cross-links and as a reinforcing filler material. The broad choice of chemical compositions possible in polyurethane systems and the subsequent wide range of physical properties exhibited has prompted a great deal of research in this area.[29–31]

Experimental Section

The samples used in this study were prepared by a standard two-step solution polymerization. Methylene bis(*p*-phenyl isocyanate) (MDI) (Eastman Kodak Co.) was purified by a double filtration of the melt under nitrogen. A mixture of the perdeuterated and hydrogenous poly(tetramethylene oxide) (PTMO) was dried for 24 h at 70 °C under vacuum. The hydrogenous PTMO used was Du Pont Teracol 1000. The d-PTMO was synthesized by a ring-opening polymerization of perdeuterated tetrahydrofuran. The excess amount of MDI and the PTMO mixture were reacted in dimethylacetamide (DMAc) solution, 30% by volume of reactants, for 3 h at 70 °C under nitrogen. The percentage of fully deuterated PTMO chains in the various samples was 0, 3, 5, 10, 20, and 30% of the total number of PTMO segments. Stannous octoate catalyst (M & T Chemicals Catalyst T-9, 0.15% by weight) was used to promote the reaction. The chain extender, 1,4-butanediol (Aldrich Chemicals), was vacuum distilled prior to use. After the initial isocyanate end capping of the polyol had occurred, the chain extender was added to complete the polymerization. The molar composition of these materials was 3 mol of MDI, 2 mol of butanediol, and 1 mol of polyol soft segment. After an additional reaction time of 2 h at 70 °C, the polymers were precipitated from the DMAc solution with water. The samples were then dried under vacuum for 1 week at 70 °C. The specimens for the SANS experiments were compression molded disks 3 cm in diameter and 1–2 mm thick. The samples were molded at 160 °C and 20 MPa for 15 min, and then were allowed to slowly cool to room temperature. The samples were then stored at room temperature in a desiccator until the scattering experiments were performed.

Sample Characterization

The deuterated PTMO prepolymer was characterized by using ^2H NMR, gel permeation chromatography, and a recently developed high-performance liquid chromatography (HPLC) technique that has been found to work extremely well for polyether glycols of low molecular weight.[32] The ^2H NMR spectrum indicated a molecular weight of 960. The GPC curve gave a number-average molecular weight around 1000. The HPLC yielded $\bar{M}_n$ = 1013, $\bar{M}_w$ = 1440, and $\bar{M}_z$ = 1990.

The polyurethane samples were characterized by differential scanning calorimetry (DSC) and small-angle X-ray scattering (SAXS). The DSC thermograms were obtained on a Perkin-Elmer DSC-II equipped with an automatic data acquisition and analysis package. The SAXS data were obtained with an Elliot GX-21 15-kW rotating copper anode generator and a Kratky compact camera. The scattering data were collected with a linear position sensitive detector coupled to a multichannel analyzer and interfaced to a PDP 11-23 microprocessor for data analysis. The X-ray data were desmeared by the method of Lake[34] and corrected for absolute intensity by

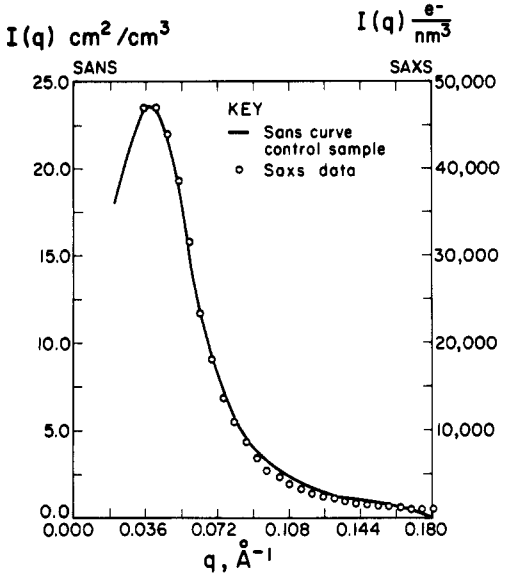

Figure 2. Comparison of the SAXS and SANS absolute scattering intensity data.

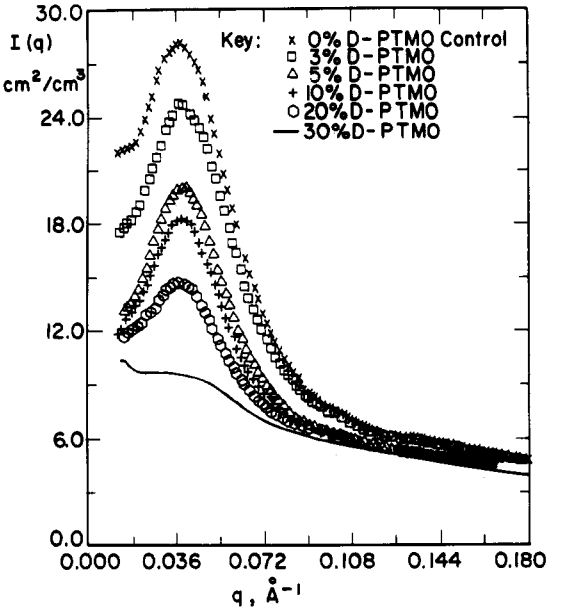

Figure 3. Absolute SANS scattering data for the series of polyether–polyurethane block copolymers.

reference to a Lupolen standard.

The DSC thermograms showed the soft segment glass transition temperature to be −41 ± 2 °C for all of the samples. A small endotherm was seen for all samples at around 60 °C, similar to results reported by Van Bogart.[28] This endotherm was ascribed to some short-range ordering of the hard domains. Thermal analysis suggests that these samples have a similar phase composition but does not give direct evidence for similar morphologies in the set of samples.

A comparison of the small-angle neutron scattering data for the nondeuterated control sample and the SAXS data for the 20% d-PTMO sample are shown in Figure 2. The agreement in the data is excellent, giving direct evidence for similarity of microstructure. The SAXS curves from the other samples match very well over most of the range of q. At very low angles, for most of the samples, the SAXS curves have a high level of anomalous scattering. However, in the important tail region, the curves match almost exactly. From the SAXS data, it can be assumed that the set of samples possesses a consistent morphology, with only slight variation between the individual samples.

Results and Discussion

The small-angle neutron scattering data for each of the samples were obtained at the National Bureau of Standards test reactor. The data were normalized for sample scattering volume and corrected for absolute intensity by using the completely incoherent scattering from a 1-mm-thick water sample as a reference standard. The multiple scattering from water was corrected for by using established techniques. According to Goyal et al.,[33] the effects of multiple scattering from the polymer sample for most typical experiments are negligible. Hence, the problem of multiple scattering by the sample was ignored. The nominal wavelength used in the experiment was 5.5 Å. The collimation apertures had a diameter of 1.2 cm. The distance between the collimation apertures was 360 cm, as was the sample-to-detector distance. The total accumulated counts were high enough such that the standard deviation of the counts per channel at q values less than 0.1 Å^{-1} was less than 6% of the total counts in a given channel. The counting time was approximately 6 h per sample.

The absolute intensity corrected scattering curves for the set of samples are shown in Figure 3. Before discussing this data, it is necessary to account for the various smearing effects in SANS that confound the raw data. The two most prominent smearing effects are wavelength polydispersity smearing and collimation geometry smearing. While these two effects are not strictly independent of each other, for simplicity they will be treated as such, as they do have only a small effect on each other.

Wavelength polydispersity smearing arises from the fact that while the data is gathered at some nominal value of the incident wavelength, λ_0, contributions to the scattering at a given q value are made from all of the wavelengths present. With X-rays, this is not a problem, since the X-ray beam is fairly monochromatic, being related to the quantum electronic properties of the X-ray source. However, neutrons used for scattering eminate from a source that is very broadband, thus a particular wavelength has a fairly low intensity. Sharp monochromatization of this source will lead to an unacceptably low incident beam strength. Because of the intensity problem, neutron beams typically have a fairly large wavelength polydispersity, and some smearing inevitably takes place. The wavelength polydispersity smearing can be expressed as

$$\tilde{I}(q)_{\lambda_0} = \int_0^\infty f(\lambda) I\left(\frac{q\lambda_0}{\lambda}\right) d\lambda \qquad (1)$$

where $\tilde{I}(q)_{\lambda_0}$ is the observed, smeared intensity at q, where q is the magnitude of the scattering vector determined at a nominal wavelength λ_0, $q = 4\pi/\lambda \sin\theta$, $I(q)$ is the real scattering intensity, λ is the actual wavelength, and $f(\lambda)$ is the wavelength distribution function. $f(\lambda)$ obeys the following equation:

$$\int_0^\infty f(\lambda)\, d\lambda = 1 \qquad (2)$$

Figure 4a illustrates the wavelength polydispersity smearing effect. At wavelengths larger than the nominal wavelength, the actual scattering curve is shifted to lower nominal q values. For wavelengths shorter than the nominal value, the reverse is true. Because of the inverse relation between q and λ, the shifting of the intensity pattern does not cancel for symmetric wavelength distribution functions, such as the one shown in Figure 4b for the NBS facility, and hence wavelength smearing results.

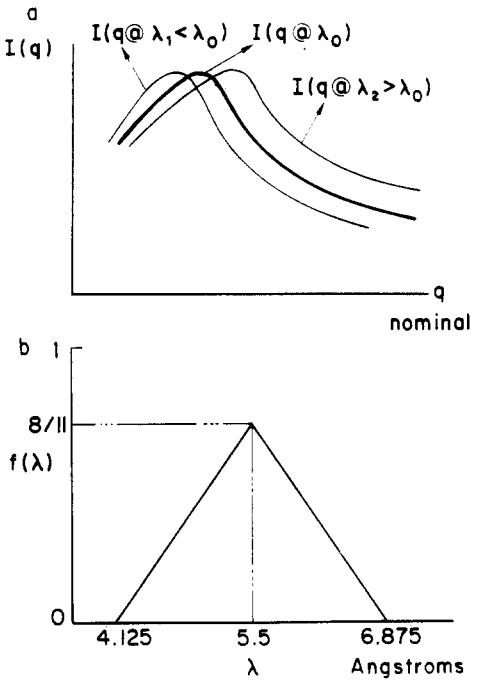

Figure 4. (a) Illustration of the effect of wavelengths larger and smaller than the nominal wavelength on the position of the scattering curve in nominal q coordinates. (b) Wavelength distribution function for the NBS facility as used in this experiment.

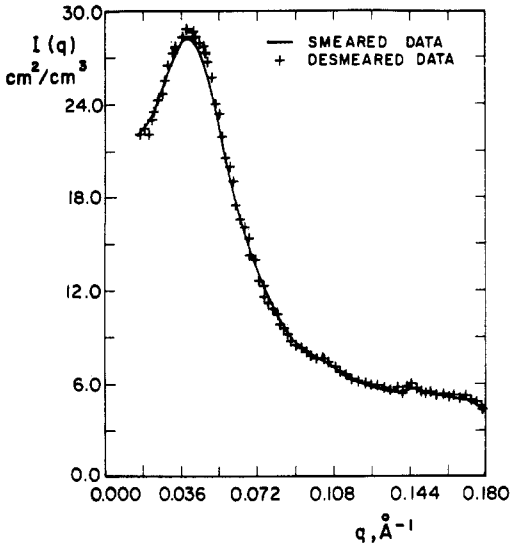

Figure 5. Results of the Lake desmearing operation for wavelength polydispersity.

By use of the geometry and specifications of the NBS monochromator, eq 1 can be rewritten as

$$\tilde{I}(q)_{\lambda_0} = \int_{4.125}^{5.5} I\left(\frac{q\lambda_0}{\lambda}\right)\left[\frac{64}{121}(\lambda - 4.125)\right] d\lambda - \int_{5.5}^{6.875} I\left(\frac{q\lambda_0}{\lambda}\right)\left[\frac{64}{121}(\lambda - 6.875)\right] d\lambda \quad (3)$$

Integral equations of this type can often be solved numerically by the iterative method of Lake.[34] Figure 5 shows the results of this desmearing operation on the control sample. Since this sample has the sharpest peak, any smearing effects present will be more pronounced with this sample than with the others. However, essentially no difference is seen between the wavelength smeared and desmeared scattering curves, except that the desmeared curve appears to have more noise. This is due in part to the numerical methods used to solve eq 3, namely the cubic polynomial spline evaluation and the Simpson integration technique. From this exercise, one sees that the wavelength polydispersity smearing problem, at least for wavelength distributions that are smooth and symmetric around the nominal wavelength, is not important. Since this is true for the NBS machine, which has a fairly large polychromaticity, it will also be true for those facilities that have a narrower wavelength distribution.

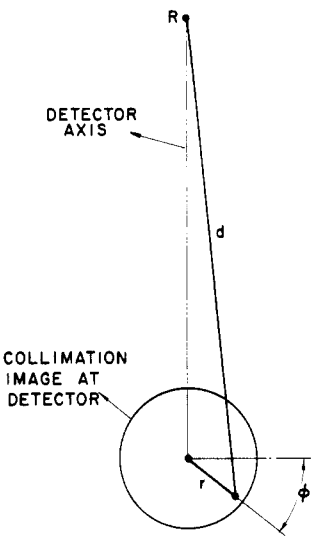

Figure 6. Illustration of the collimation smearing effect. The actual distance traveled by the scattered radiation depends on the position within the collimation image from which the ray originated.

The collimation smearing effect arises from the finite size of the collimation apertures. With infinitesimally small pinholes, there is no smearing. However, the 1.2-cm diameter apertures used in this experiment are not pinholes, and some smearing takes place. An analogous problem exists in X-ray scattering for certain scattering geometries, such as the infinite slit collimation and the Kratky geometry.

By use of the techniques developed for slit smearing in small-angle X-ray scattering, the collimation smearing equation can be derived and solved using Lake's method. Figure 6 shows the image of the collimation apertures on the detector plane. The size of this region depends on the distance between apertures, the size of the apertures, and the sample to detector distance. Considering one direction along the detector, the scattering at point R on the detector is composed of contributions from each point within the image of the apertures at the detector. This can be written as an integral over the image area where the real intensity at a given distance is weighted by the beam intensity within the aperture image.

$$\tilde{I}(R) = \int_0^{2\pi}\int_0^{\infty} W(r,\phi)I(d)r\, dr\, d\phi \quad (4)$$

In this expression, $\tilde{I}(R)$ is the observed, smeared intensity at the position R along the detector, $W(r,\phi)$ is the beam intensity weighting function within the aperture image, $I(d)$ is the real scattering intensity at a distance d, a distance that is measured in the same plane as R, and r and ϕ are the polar coordinates describing the circular collimation aperture image. d is related to R, r, and ϕ by

$$d = [r^2 + R^2 - 2rR\sin\phi]^{1/2} \quad (5)$$

$W(r,\phi)$ has the following property

$$\int_0^{2\pi}\int_0^{\infty} W(r,\phi)r\, dr\, d\phi = 1 \quad (6)$$

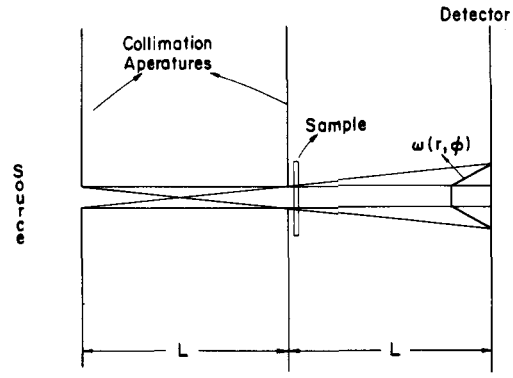

Figure 7. Illustration of the optical geometry used in this experiment. From this diagram and eq 6, the weighting function $W(r,\phi)$ can be derived.

and can be determined from the scattering geometry, as illustrated in Figure 7. This figures shows the two-dimensional profile of the optical configuration used in this experiment. The intensity of the main beam at the detector due to the collimation geometry is in two dimensions trapezoidal in shape, corresponding to the umbra and penumbra of the collimation shadows. In three dimensions, the weighting function is a truncated cone. For the NBS facility as it was used in this experiment, $W(r,\phi)$ can be expressed as

$$W(r,\phi) = \frac{3}{13\pi}\left(\frac{1}{R_0^2}\right) \qquad r \le R_0$$

$$= \frac{3}{26\pi}\left(\frac{1}{R_0^3}\right)(3R_0 - r) \qquad R_0 \le r \le 3R_0 \qquad (7)$$

where R is the radius of the apertures, 0.6 cm for the experiments described in this contribution. $W(r,\phi)$ has no ϕ dependence and thus can be denoted as $W(r)$. The collimation smearing equation can then be written as

$$\tilde{I}(R) = \int_0^{2\pi}\int_0^{R_0} \frac{3}{13\pi}\left(\frac{1}{R_0^2}\right) \times I(\{r^2 + R^2 - 2rR\sin\phi\}^{1/2})r\,dr\,d\phi + \int_0^{2\pi}\int_{R_0}^{3R_0} \frac{3}{26\pi}\left(\frac{1}{R_0^3}\right) \times (3R_0 - r)I(\{r^2 + R^2 - 2rR\sin\phi\}^{1/2})r\,dr\,d\phi \quad (8)$$

This equation is applicable to scattering geometries where the collimation apertures are the same size and where the distance between apertures is equal to the distance from the last aperture to the detector. Figure 8 shows the results of solving eq 8 for $I(d)$ by using Lake's procedure. As in the case for wavelength polydispersity smearing, the effect of collimation smearing on the experimental data is small. When both wavelength and collimation corrections are made to the data, the same conclusion is reached. Thus, for most common SANS geometries, the collimation approximates a pinhole fairly well, since the smearing for the NBS facility is expected to be worse than that for machines with better collimation. Similar conclusions were reached by Wignall et al.[35] by applying a Monte Carlo simulation and analysis to the circular collimation smearing problem.

The smearing effects in a typical SANS experiment using circular collimation have been shown to be negligible. Thus, the raw data shown in Figure 3 can be used for further analysis without desmearing. The absolute level

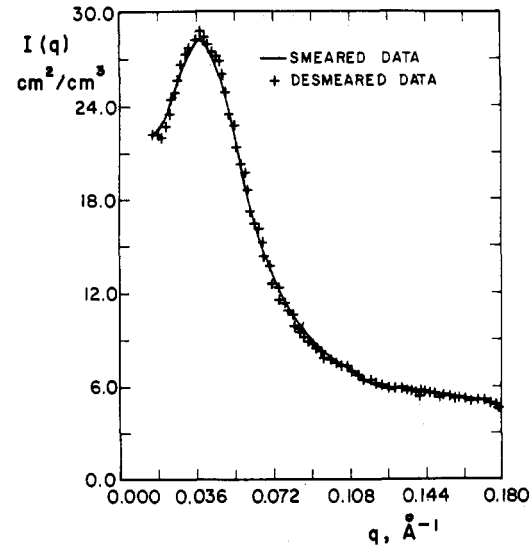

Figure 8. Results of the Lake desmearing process for the collimation smearing effect.

Table I

sample	β(soft segment), (cm/cm³) × 10^{-9}	β(hard segment), (cm/cm³) × 10^{-9}
0% d-PTMO	2.02	25.22
3% d-PTMO	3.93	25.13
5% d-PTMO	5.19	25.18
10% d-PTMO	8.40	25.18
20% d-PTMO	14.86	25.05
30% d-PTMO	21.43	24.85

of the scattering in each of the samples decreases as the level of deuteration increases. This is because as the degree of deuterium substitution is increased, the coherent scattering length density of the soft phase increases. Since the interphase coherent scattering is proportional to the square of the difference in coherent scattering length densities between the phases, reducing this difference by increasing the value for the soft phase causes a lower level of interphase coherent scattering. Table I lists the values for the coherent scattering length densities for each phase for each sample, assuming that no phase mixing occurs. These values are calculated from the densities of the samples and from the density of the PTMO homopolymer. One can calculate that at a deuterated soft segment content of 32.5%, the hard and soft phase coherent scattering length densities will be equal. Under these conditions, no interphase scattering occurs and only the single-chain scattering appears in the coherent portion of the total scattering. The sample containing 30% d-PTMO chains approximates this condition. From Figure 3, it is seen that little structure is present in the scattering curve, indicative of a low level of interphase scattering.

To extract the single-chain scattering from the data, the equation of Koberstein[17] was used.

$$[R_L(q) - R_{L,BKg}(q)] - \left[\frac{\beta_A - x\beta_{BD} - (1-x)\beta_{BH}}{\beta_A - \beta_{BH}}\right]^2 [R_U(q) - R_{U,BKg}(q)] = \frac{4\pi}{V_s}(b_{BD} - b_{BH})^2 N_{BT} Z_B^2 x(1-x)P_B(q) \quad (9)$$

In this equation, $R_L(q)$ and $R_U(q)$ are the total scattering terms from the labeled and unlabeled control samples respectively, $R_{L,BKg}(q)$ and $R_{U,BKg}(q)$ are the corresponding

background terms, β_A is the coherent scattering length density of phase A, the hard phase in this experiment, β_{BH} and β_{BD} are the coherent scattering length densities for the hydrogenous and deuterated phase B, the soft phase in this experiment, and x is the fraction of "B" chains that are deuterated. The volume of the sample that is illuminated by the incident beam is denoted V_s, b_{BH} and b_{BD} are the monomer coherent scattering length for the hydrogenous and deuterated "B" monomers, N_{BT} is the total number of "B" chains present in the scattering volume, Z_B is the degree of polymerization of the "B" chains, and $P_B(q)$ is the single-chain scattering function for the "B" segments. $P_B(q)$ describes the scattering that arises from the contrast difference between the labeled and unlabeled soft segment chains. The above equation involves the subtraction of the interphase portion of the coherent scattering by performing a weighted subtraction of the scattering from an unlabeled sample from the scattering from a partially labeled sample. The weighting factor is the square of the ratio of the difference in coherent scattering length densities between the two phases for the labeled and unlabeled samples. This equation was derived without making any assumptions regarding phase purity and phase mixing. One has to consider this when discussing polyurethane systems, as these materials exhibit a substantial degree of phase mixing. When phase mixing does occur, additional interchain scattering terms appear in eq 9, for example the interchain scattering arising from the correlations between the soft segments in the soft phase and the hard segments dissolved in the soft phase. Fortunately, for small degrees of intersegmental mixing, these additional interchain scattering contributions are small and hence can be ignored. Also, the phase contrast weighting factor can be calculated by using the pure-phase coherent scattering length densities. The results obtained are identical with those obtained when the coherent scattering length densities are calculated by using mixed phases. Equation 9 was therefore used without correction for phase mixing to analyze the data in this experiment, keeping in mind the limitations imposed by this approximation. Thus there is no need to know the exact compositions of the individual phases, quantities that are often difficult or impossible to determine accurately.

Equation 9 can be modified to allow the extraction of the single-chain scattering from two labeled samples containing different levels of deuteration. The resulting equation is

$$[R_1(q) - R_{1,inc}] - \left(\frac{\beta_{A1} - \beta_{B1}}{\beta_{A2} - \beta_{B2}}\right)^2 [R_2(q) - R_{2,inc}] = \frac{4\pi}{V_{s1}}(b_{BD} - b_{BH})^2 N_{BT1} Z_B^2 x_1(1 - x_1) P_B(q) - \left(\frac{\beta_{A1} - \beta_{B1}}{\beta_{A2} - \beta_{B2}}\right)^2 \frac{4\pi}{V_{s2}}(b_{BD} - b_{BH})^2 N_{BT2} Z_B^2 x_2(1 - x_2) P_B(q) \quad (10)$$

where the samples are designated 1 and 2 and the terms in this equation correspond to those in eq 9. β_{A1} and β_{B1} refer to the coherent scattering length densities of the hard and soft pure phases for sample 1, and β_{A2} and β_{B2} correspond to the values for sample 2. The background scattering terms have been replaced by the incoherent scattering terms. Koberstein[17] has calculated that for typical polymer systems, the incoherent portion of the scattering completely dominates the other contributions to the background scattering. Use of this equation with the series of samples in this experiment allows confirmation of the single-chain scattering function obtained through repeated checks using different sample pairs. Thus this provides an internal check on the consistency of the data analysis.

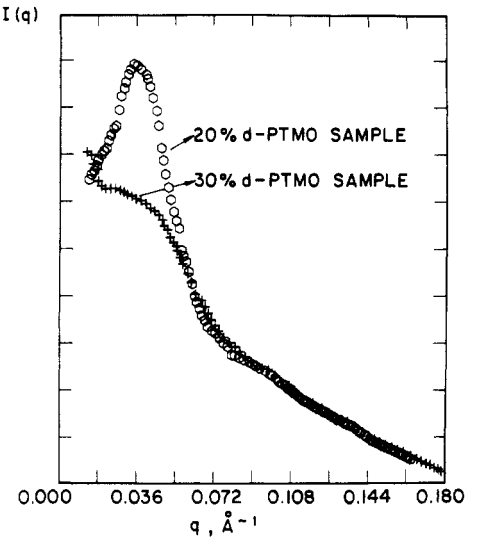

Figure 9. Single-chain scattering functions for the samples containing 20% and 30% d-PTMO.

Figure 9 shows the single-chain scattering functions obtained from the samples containing 20 and 30% labeled d-PTMO chains. Application of eq 9 and 10 gave essentially identical results for all combinations of materials containing the 20% and 30% samples. It is interesting to note the presence of the peak in the 20% d-PTMO sample. This peak indicates the presence of some interphase scattering. This does not imply the failure of eq 9 and 10, but rather points out the main difficulty in applying this technique. The problem is that it is very difficult to obtain two samples with different levels of labeling that possess exactly the same microstructure. When this microstructure does not correspond exactly, small discrepancies arise in the raw scattering curves, thus leading to artifacts in the data. This is the problem with the 20% d-PTMO curve shown in Figure 9. Similar problems were encountered upon trying to extract the single-chain scattering from the 10% labeled sample.

For the samples containing 3% and 5% labeled chains, the single-chain scattering function could not be extracted. There are several reasons for this. First, the single-chain scattering is obtained as the difference between two large numbers. At low levels of deuteration, the statistical noise in the original data tends to mask the contribution from the single-chain scattering. Second, especially at low levels of deuteriolabeling, slight differences in microstructure will lead to major difficulties in the extraction of the single-chain scattering data. Lastly, since the level of single-chain scattering in the coherent part of the total scattering is proportional to the product $x(1 - x)$, at small values of x the contribution of the single-chain scattering to the total will be small. Because of these reasons, only the samples with the higher levels of deuteration provide usable single-chain scattering functions.

To extract the radius of gyration of the soft segment, the method of Guinier[24] was used. Guinier plots for the single-chain scattering functions obtained from the 10, 20, and 30% d-PTMO samples are shown in Figure 10. The range of q plotted was chosen so that the product $q \times R_g$ was as small as possible, less than 1.5, yet q was large enough so that the residual interphase scattering from the 10% and 20% samples did not affect the data analysis. This range of q values has been shown to give reasonably accurate values for the radius of gyration.[20,23,25] The value

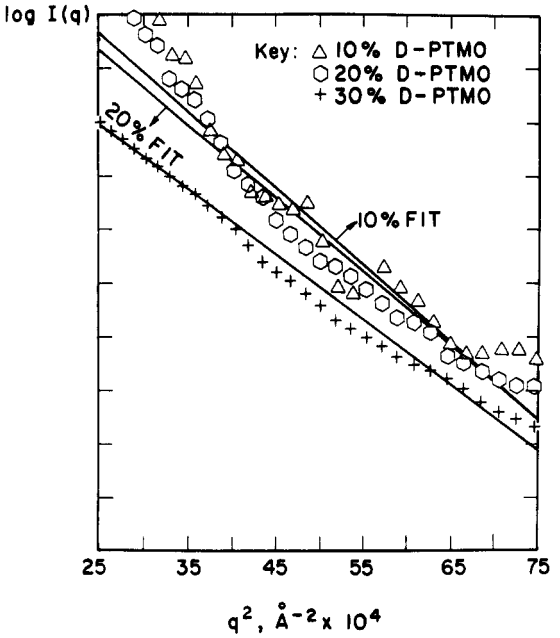

Figure 10. Guinier plot of the single-chain scattering functions obtained with the 10%, 20%, and 30% d-PTMO samples.

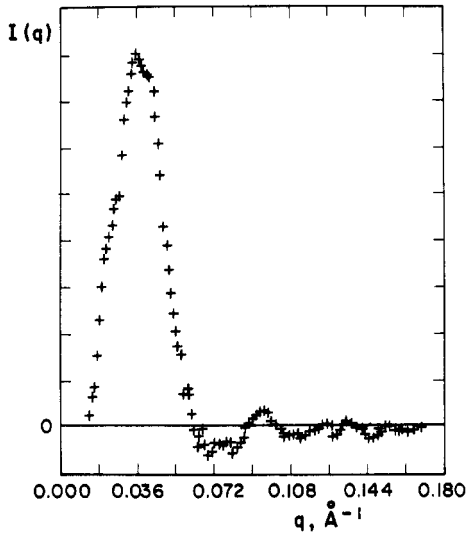

Figure 11. Difference plot of the 20% d-PTMO single chain scattering function minus the 30% d-PTMO single-chain scattering function.

of q above which the interphase scattering vanishes was chosen with the aid of the plot shown in Figure 11. This figure is a difference plot of the single-chain scattering functions obtained from the 20% and 30% d-PTMO samples. The point at which the difference plot reaches zero is the point at which interphase scattering becomes negligible. Simply stated, the reason for this is that the particles which give rise to the interphase scattering (the individual domains) are substantially larger than the particles that cause the interchain scattering. Hence, the scattering from the phases drops off much more rapidly than the scattering from the soft segment chains. The z-average radii of gyration obtained from the slope of the Guinier plot for each sample are 22.2 ± 1.4 Å, 21.4 ± 1.2 Å, and 21.0 ± 0.59 Å for the 10, 20, and 30% d-PTMO samples, respectively. The error limits are for a 95% confidence limit as determined by a standard t-test of the linear regression analysis. By comparison, a number-average radius of gyration of 11.7 Å has been reported by Kurata et al.[36] and others[37,38] for PTMO of 1000 molecular weight in a Θ solvent as determined by limiting viscosity methods.

The weight-average molecular weight of the soft segment can be determined by SANS using the zero q intercept of the Guinier plot. The expression for the weight-average molecular weight is[39]

$$\bar{M}_w = I(0)/C_H C_D K_N \tag{11}$$

where $I(0)$ is the intercept from the Guinier plot, C_D and C_H are the concentrations of the deuterated and hydrogenous monomers, respectively, and K_N is a calibration constant given by

$$K_N = \rho N_0 \left[\frac{\nu x (b_D - b_H)}{M_0} \right]^2 \tag{12}$$

Here ρ is the sample density, N_0 is Avogadro's number, ν is the number of replaceable hydrogen atoms per monomer, x is the fraction of deuteration, b_D and b_H are the monomer coherent scattering lengths for the deuterated and hydrogenous monomers, and M_0 is the monomer molecular weight. Use of eq 11 and 12 along with the appropriate experimental values leads to a molecular weight of 1850 ± 150, with a t-test confidence limit of 95%, compared to an $\bar{M}_w$ of 1440 as determined by HPLC. These results are in good agreement considering the errors present in the SANS experiment and in the HPLC experiment at low molecular weights. In particular, the additional interchain scattering due to the small amounts of interphase mixing present will cause the value of the Guinier plot intercept to increase, thereby yielding an apparent molecular weight somewhat higher than the actual value.

Two types of polydispersity corrections may have to be taken into account which modify the experimentally determined radius of gyration in order to compare it to literature values. Tangari et al.[22] and Boue et al.[40] have discussed the problems associated with having dissimilar chain lengths and distributions between the labeled and unlabeled chains in the determination of the chain conformation. For samples which have reasonably similar labeled and unlabeled chain molecular weights and distributions, these corrections are quite small.

Since the radius of gyration determined from a Guinier plot is a z-average value, the number-average value must be obtained from the z-average value and the molecular weight distribution in order to properly compare the results with literature values. As is commonly done in light scattering, a Schulz[41] distribution was used for the size distribution of the soft segments.

$$w(M) = \frac{y^{h+1}}{\Gamma(h+1)} M^h e^{-yM} \tag{13a}$$

where

$$y = \frac{h}{\bar{M}_n} = \frac{h+1}{\bar{M}_w} = \frac{h+2}{\bar{M}_z} \tag{13b}$$

In this equation, $w(M)$ is the weight fraction of species with a molecular weight of M, $\Gamma(x)$ is the Γ function, and h is a measure of the polydispersity of the polymer. Large values of h correspond to a narrow molecular weight distribution, and a value of h equal to 1 corresponds to the most probable distribution. For the deuterated soft segments used in this experiment, $\bar{M}_n$ = 1013, $\bar{M}_w$ = 1440, and $\bar{M}_z$ = 1990, as measured by high-performance liquid chromatography. These molecular weights correspond to an h value of about 2.21. From the Schulz distribution and the definitions of number, weight, and z averages, the

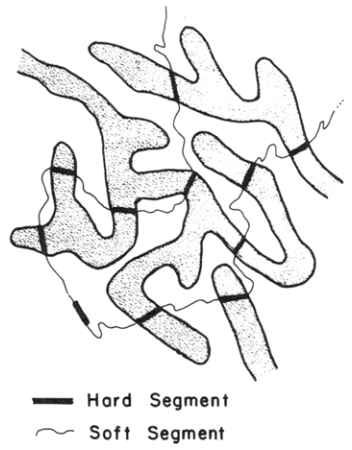

Figure 12. Model of a single polyurethane block copolymer chain as it traverses the microstructure of the system.

following expressions describing the interrelation between the various average radii of gyration can be derived.

$$\langle R_g^2 \rangle_z = \langle R_g^2 \rangle_n \left(\frac{h+2}{h} \right) \tag{14a}$$

$$\langle R_g^2 \rangle_z = \langle R_g^2 \rangle_w \left(\frac{h+2}{h+1} \right) \tag{14b}$$

When this conversion is applied to the z-average values previously mentioned, the resulting number-average radii of gyration become 16.1 ± 1.0 Å, 15.5 ± 0.87 Å, and 15.2 ± 0.43 Å for the 10, 20, and 30% d-PTMO samples. Compared to the literature value of 11.7 Å in a Θ solvent, this represents an expansion of about 35% in the block copolymer. Therefore, the chains are in a somewhat extended conformation in this lamellar polyurethane block copolymer, with the soft segments extending between the lamellar hard domains, similar to the styrene blocks in the lamellar styrene/isoprene copolymer as reported by Hadziioannou et al.[23] The model first proposed by Estes[42] shown in Figure 12, also seems appropriate in describing the chain trajectory for this polyurethane block copolymer.

Conclusions

Three principal conclusions can be drawn from the results of this study. First, the soft segment chains in this polyurethane system are in a somewhat extended conformation. This is due to the anchoring of the chain ends at the hard phase/soft phase interface. The phase separation that occurs upon solidification tends to extend the soft segment chains. Similar results were obtained for the styrene block in a styrene/isoprene block copolymer,[23] the only other lamellar system for which the chain conformation has been reported. These results are significantly different from those reported for systems having spherical domains. In these systems, the segments in the spherical domains are reported to have a random coil conformation,[20,25] though the conformation of the chains in the matrix of these systems has not been reported.

Second, the single-chain scattering function is most easily obtained by selecting samples with a level of labeling such that the individual phases are contrast matched and no interphase scattering occurs. From eq 9, this condition is true when

$$\beta_A - x\beta_{BD} - (1-x)\beta_{BH} = 0 \tag{15}$$

In the system studied, application of eq 15 leads to a desired sample with a high level of deuteration (32.5%). This high level is advantageous in producing a strong signal due to the interchain scattering, and hence better counting statistics with less noise. The phase contrast method is superior in that it eliminates the problem of trying to exactly match the microstructure of two different samples, as is required by the subtraction technique. Matching this microstructure can be very difficult.

Finally, the effects of wavelength polydispersity and collimation smearing on SANS data analysis have been investigated. For the NBS facility, neither smearing effect is significant.

Acknowledgment. We acknowledge partial support of this work by the Polymer Section of the Division of Materials Research of the National Science Foundation under Grant No. DMR 81-06888. We also thank Dr. Jeffrey Koberstein of Princeton University for valuable discussions concerning the experiments reported on in this contribution.

References and Notes

(1) D. G. H. Ballard, G. D. Wignall, and J. Schelten, *Eur. Polym. J.*, **9**, 965 (1973).
(2) P. J. Flory, "Principles of Polymer Science", Cornell University Press, Ithaca, New York, 1951.
(3) G. D. Wignall, D. G. H. Ballard, and J. Schelten, *Eur. Polym. J.*, **10**, 801 (1974).
(4) R. G. Kirste, W. A. Kruse, and J. Schelten, *J. Makromol. Chem.*, **162**, 299 (1973).
(5) R. G. Kirste and B. R. Lehnen, *Makromol. Chem.*, **177**, 1137 (1976).
(6) R. G. Kirste, W. A. Kruse, and K. Ibel, *Polymer*, **16**, 645 (1975).
(7) J. S. Higgins and R. S. Stein, *J. Appl. Crystallogr.*, **11**, 346 (1978).
(8) R. W. Richards in "Developments in Polymer Characterization", Applied Science Press, London, 1978.
(9) J. Schelten, G. D. Wignall, D. G. H. Ballard, and G. W. Longman, *Polymer*, **18**, 1111 (1977).
(10) D. Sadler and A. Keller, *Macromolecules*, **10**, 1128 (1977).
(11) D. G. H. Ballard, G. W. Longman, T. L. Crowley, and A. Cunningham, *Polymer*, **20**, 399 (1979).
(12) J. Schelten, G. D. Wignall, and D. G. H. Ballard, *Polymer*, **15**, 682 (1974).
(13) D. G. H. Ballard, A. N. Burgess, A. Nevin, P. Cheshire, and G. W. Longman, *Macromolecules*, **13**, 677 (1980).
(14) G. Allen and T. Tanaka, *Polymer*, **19**, 71 (1978).
(15) G. C. Summerfield, J. S. King, and R. Ullman, *J. Appl. Crystallogr.*, **11**, 548 (1978).
(16) J. H. C. Ching and S. Krimm, *Macromolecules*, **8**, 894 (1975).
(17) J. T. Koberstein, *J. Polym. Sci., Polym. Phys. Ed.*, **20**, 593 (1982).
(18) S. N. Jahshan and G. C. Summerfield, *J. Polym. Sci., Polym. Phys. Ed.*, **18**, 1859 (1980).
(19) S. N. Jahshan and G. C. Summerfield, *J. Polym. Sci., Polym. Phys. Ed.*, **18**, 2145 (1980).
(20) R. W. Richards and J. L. Thomason, *Polymer*, **22**, 581 (1981).
(21) N. T. Notley and P. J. W. Debye, *J. Polym. Sci.*, **17**, 99 (1955).
(22) C. Tangari, J. S. King, and G. C. Summerfield, *Macromolecules*, **15**, 132 (1982).
(23) G. Hadziioannou, C. Picot, A. Skoulios, M. L. Ionescu, A. Mathis, R. Duplessix, Y. Gallot, and J. P. Lingelser, *Macromolecules*, **15**, 263 (1982).
(24) A. Guinier and G. Fournet, "Small Angle Scattering of X-Rays", Wiley, New York, 1955.
(25) F. S. Bates, C. V. Berney, R. E. Cohen, and G. D. Wignall, *Polymer*, **25**, 519 (1983).
(26) A. Z. Akcasu, G. C. Summerfield, S. N. Jahshan, C. C. Han, C. U. Kim, and H. Yu, *J. Polym. Sci., Polym. Phys. Ed.*, **18**, 865 (1980).
(27) G. D. Wignall, R. W. Hendricks, W. C. Koehler, J. S. Lin, M. P. Wai, E. L. Thomas, and R. S. Stein, *Polymer*, **22**, 886 (1981).
(28) J. W. C. Van Bogart, Ph.D. Dissertation, Department of Chemical Engineering, University of Wisconsin—Madison, 1981.
(29) S. L. Cooper and G. M. Estes, Eds., "Multiphase Polymers", American Chemical Society, Washington, DC, 1979, Adv. Chem. Ser. No. 176, p3.
(30) P. E. Gibson, M. A. Vallance, and S. L. Cooper in "Developments in Block Copolymers", I. Goodman, Ed., Elsevier, London, 1982, Appl. Sci. Ser. p 217.
(31) C. Hepburn, "Polyurethane Elastomers", Applied Science Publishers, Elsevier, London, 1982.
(32) G. D. Andrews, A. Vatvars, and G. Pruckmayr, *Macromolecules*, **15**, 1580 (1982).

(33) P. S. Goyal, J. S. King, and G. C. Summerfield, *Polymer*, **24**, 131 (1983).
(34) J. A. Lake, *Acta Crystallogr.*, **23**, 191 (1967).
(35) G. D. Wignall, presented at the American Physical Society Meeting, Los Angeles, CA, March, 1983.
(36) M. Kurata, H. Utiyama, and K. Kamada, *Makromol. Chem.*, **88**, 281 (1965).
(37) K. Bak, E. Elefante, and J. E. Mark, *J. Phys. Chem.*, **71**, 4007 (1967).
(38) J. M. Evans and M. B. Huglin, *Makromol. Chem.*, **127**, 141 (1969).
(39) D. G. H. Ballard, P. Cheshire, E. Janke, A. Nevin, and J. Schelten, *Polymer*, **23**, 1875 (1982).
(40) F. Boue, M. Nierlich, and L. Liebler, *Polymer*, **23**, 29 (1982).
(41) G. V. Schulz, *Z. Phys. Chem., Abt. B*, **B43**, 25 (1939).
(42) G. M. Estes, Ph.D. Dissertation, Department of Chemical Engineering, University of Wisconsin—Madison, 1971.

Study of the Solid-State Crosspolymerization of Poly(1,11-dodecadiyne) through Magic-Angle Carbon-13 NMR

John R. Havens, M. Thakur, Jerome B. Lando, and Jack L. Koenig*

Department of Macromolecular Science, Case Western Reserve University, Cleveland, Ohio 44106. *Received October 18, 1982*

ABSTRACT: High-resolution carbon-13 NMR spectra of solid poly(1,11-dodecadiyne) before and after γ-irradiation are reported. The crosspolymerization reaction is shown to result in a conjugated backbone characterized by the acetylenic structure instead of by the butatriene possibility. Resolution of amorphous and crystalline contributions to the spectra is demonstrated. Evidence that crosspolymerization occurs predominantly in crystalline domains is also discussed.

I. Introduction

The polymerization of diacetylene crystals has generated considerable interest as a solid-state reaction which occurs systematically throughout the crystal lattice.[1,2] Under appropriate conditions, the monomer can be converted to a macroscopic polymeric single crystal, the chains of which are fully conjugated. The polymerization can be initiated in several ways, including γ-irradiation,[1,3] UV irradiation,[4,5] heat,[6,7] and pressure. Recently, these reactions have been extended to include polymers as the starting material prior to irradiation.[8,9] The initial polymer (or "macromonomer") contains diacetylene groups in its repeat unit, which can react in a manner similar to that observed for the diacetylene monomers. Exposure to high-energy radiation initiates the reaction of diacetylene groups belonging to consecutive macromonomer chains and results in a systematic sheetlike structure which is covalently bonded in two dimensions. This procedure has been termed crosspolymerization in order to distinguish it from the random cross-linking which many polymers experience upon irradiation. The macromonomer which we have investigated in this work is poly(1,11-dodecadiyne):

$$+(CH_2)_8-C\equiv C-C\equiv C+_x$$

A diagram of its crosspolymerization, as deduced from previously reported electron diffraction results,[9] is presented in Figure 1.

While diffraction work characterizes fully the molecular structure in the crystalline regions, there remain interesting questions to be answered. One of these concerns the electronic structure along the direction of crosspolymerization. Two forms have been observed in the polymerization of diacetylene monomers, the acetylenic (enyne) and butatriene structures:[10-14]

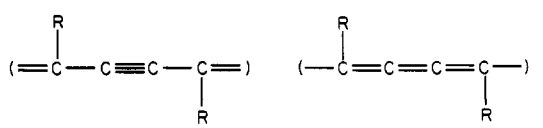

acetylenic butatriene

Bond lengths from diffraction work can be used to discriminate between these two, but a more sensitive indication is desirable. This is true particularly for the crosspolymerized materials, where relatively few unique diffraction maxima are recorded. Another question deals with the semicrystalline nature of the macromonomer; the influence of the amorphous component on crosspolymerization is not well understood presently. Such consideration is not necessary in the polymerization of diacetylene monomers, which are completely crystalline under normal conditions.

These questions can be answered in part by the use of recently developed high-resolution techniques for ^{13}C NMR in rigid solids. The techniques consist of magic-angle spinning[15] and high-power decoupling[16] to coherently average certain line-broadening interactions. Cross polarization[17,18] from protons to carbons is also employed for sensitivity enhancement. Simultaneous use of these procedures can result in spectra of solid polymers in which chemically distinct carbon types have separately resolved resonances.[19,20] This capability is particularly attractive for the analysis of crosspolymerized poly(1,11-dodecadiyne), whose network structure makes it insoluble and infusible.

II. Experimental Section

The macromonomer was prepared by oxidative coupling of 1,11-dodecadiyne with a copper–pyridine catalyst. Details of the synthesis have been published previously.[8,21,22] Samples were stored at −10 °C and shielded from light prior to crosspolymerization. γ-Irradiation from a ^{60}Co source (23 Mrd) was used to crosspolymerize the macromonomer. It was also discovered that for some of the unirradiated samples crosspolymerization could be induced during packing of the material in the rotor by hand. The mechanical shear associated with twisting the plunger during packing was sufficient to initiate the reaction. When the macromonomer was packed with an effort to minimize such twisting, resonances indicative of crosspolymerization were not observed.

Carbon-13 cross-polarization (CP) magic-angle spinning (MAS) spectra were recorded at 38 MHz on a modified Nicolet NT-150 spectrometer. Radio-frequency field strengths of approximately

0024-9297/84/2217-1071$01.50/0